

**IN SILICO STUDY, SYNTHESIS,  
CHARACTERISATION AND CYTOTOXICITY  
ACTIVITY OF NEW CHALCONE, PYRAZOLINE  
AND PYRIMIDINE DERIVATIVES**

**MENIER METEB MOHAMMAD ALANAZI**

**UNIVERSITI SAINS MALAYSIA**

**2021**

**MOLECULAR MODELLING, SYNTHESIS,  
CHARACTERISATION AND CYTOTOXICITY  
ACTIVITY OF NEW CHALCONE, PYRAZOLINE  
AND PYRIMIDINE DERIVATIVES**

**by**

**MENIER METEB MOHAMMAD ALANAZI**

**Thesis submitted in fulfillment of the requirements  
for the degree of  
Doctor of Philosophy**

**May 2021**

## ACKNOWLEDGEMENT

In the name of Allah, Most Gracious, Most Merciful.

All praise and glory to Allah the almighty who says: "and of knowledge, Ye have been vouchsafed but little" Al-Isra, verse (85). Peace be upon the Prophet, his companions and all who followed him until the Day of Judgment. Glory and praise are to Allah who has given me the strength, patience and knowledge, in guiding me through the challenges to finish my PhD journey.

This is the best place to admit beholden and gratitude. I would like to extend my sincere thanks and gratitude to Allah first and foremost, and then to my supervisors, Associate Professor Dr. Melati Khairuddean as main supervisor and Dr. Belal O. Al-Najjar as the field supervisor for supervising my PhD work. Their good supervision and sincere advice, guidance and continuous effort have shown great support, after Allah Almighty, and have helped me in completing my research work and finishing my dissertation conveniently.

My profound gratitude goes without exception to the School of Chemical Sciences, Universiti Sains Malaysia for extending the facilities and support in the completion of this work. My appreciation goes to Advanced Medical and Dental Institute, Universiti Sains Malaysia and Al-Ahliyya Amman University for the support in the biological analysis. All my thanks to Tabuk University for the sponsorship of this Ph.D. degree.

This thesis would never have seen the sun without the full support of my mother who, after Allah, was my greatest supporter. She has provided me with love, guidance, prayer and endless advice and wisdom which I can never repay. I wish to

express my heartfelt gratitude to my father for his encouragement, constant prayers and continuing support. I owe a lot of thanks to my husband, my companion, for his extra patience and motivation. My heartfelt thanks to my brothers, sisters and friends for their support and encouragement. May Allah reward all of them well. Finally, I am also thankful to all who have assisted me directly and indirectly in the completion of this work.

Thank you

Menier Al-anazi

October 2020

## TABLE OF CONTENTS

<b>ACKNOWLEDGEMENT</b> .....	ii
<b>TABLE OF CONTENTS</b> .....	iv
<b>LIST OF TABLES</b> .....	viii
<b>LIST OF FIGURES</b> .....	x
<b>LIST OF SCHEMES</b> .....	xv
<b>LIST OF SYMBOLS AND ABBREVIATIONS</b> .....	xvi
<b>LIST OF APPENDICES</b> .....	xxi
<b>ABSTRAK</b> .....	xxiii
<b>ABSTRACT</b> .....	xxv
<b>CHAPTER 1 INTRODUCTION</b> .....	1
1.1 Background of the study.....	1
1.1.1 Cancer .....	1
1.1.2 Epidermal Growth Factor Receptors (EGFRs) .....	3
1.1.3 Chalcones, pyrazoline and pyrimidine scaffold as anticancer agent.....	4
1.2 Problem Statement .....	5
1.3 Objectives .....	7
1.4 The scope of the study.....	8
<b>CHAPTER 2 LITERATURE REVIEW</b> .....	9
2.1 Tyrosine kinase protein-inhibitors .....	9
2.2 Chalcone as therapeutic agents .....	11
2.2.1 Synthesis of chalcone molecules.....	13
2.2.1(a) Claisen-Schmidt Condensation .....	13
2.2.1(b) Aldol Condensation .....	14
2.2.1(c) Suzuki Reaction.....	14

2.2.1(d)	Heck Reaction .....	15
2.2.1(e)	Reaction via Microwave Irradiation .....	15
2.2.1(f)	Reaction via Ultrasound Irradiation.....	16
2.2.1(g)	Reaction via solvent-free reaction .....	16
2.2.2	Anticancer activities of chalcone molecules .....	17
2.3	Molecules with pyrazoline scaffold .....	27
2.3.1	Synthesis of pyrazoline molecules .....	28
2.3.1(a)	Synthesis of pyrazoline from $\alpha,\beta$ -unsaturated Carboxylic Acid Esters .....	29
2.3.1(b)	Synthesis of pyrazoline from $\alpha,\beta$ -unsaturated Ketones .....	29
2.3.1(c)	Synthesis of pyrazoline from chalcone derivatives .....	30
2.3.2	Biological activities of pyrazoline molecules .....	30
2.4	Molecules with pyrimidine scaffold.....	37
2.4.1	Synthesis of pyrimidine molecules.....	38
2.4.1(a)	Synthesis based on the 1,3-dipolar compound and nitrogen fragment .....	38
2.4.1(b)	Synthesis based on uracil and thymine derivatives .....	39
2.4.1(c)	Synthesis based on chalcone and guanidine hydrochloride.....	39
2.4.1(d)	Synthesis based on chalcone and guanidine nitrate.....	40
2.4.1(e)	Synthesis of resin-bound pyrimidine derivatives .....	40
2.4.2	Biological Activities of Pyrimidine Molecules .....	40
2.5	Design of Target Molecules: Computer-Aided Drug Design (CADD) .....	46
2.6	Structure-Based Drug Design (SBDD) .....	48
2.6.1	Molecular Docking .....	49
2.6.2	Molecular Dynamics.....	52

<b>CHAPTER 3</b>	<b>MATERIALS &amp; METHODOLOGY</b>	<b>54</b>
3.1	Molecular Modeling and Molecular Dynamic	54
3.1.1	Molecular Docking	54
3.1.2	Molecular Dynamics (MD)	56
3.1.2(a)	Model Setup	56
3.1.2(b)	Minimisation	57
3.1.2(c)	Equilibration	57
3.1.2(d)	Production stage	57
3.1.2(e)	MM-GBSA calculation	58
3.2	Chemicals	58
3.3	Analytical methods and Instruments	59
3.3.1	Fourier Transform Infrared Spectroscopy (FT-IR)	59
3.3.2	Nuclear Magnetic Resonance Spectroscopy (NMR)	59
3.3.3	Elemental analysis	60
3.4	Synthesis methods	60
3.4.1	Synthesis of 1,3,5-tri-chalcone derivatives, S1-1 and S1-2	61
3.4.2	Synthesis of nitrilo- <i>tri</i> -(benzene-1,3,5-chalcone) derivatives, S2-1 and S2-2	63
3.4.3	Synthesis of mono-chalcone derivatives, S3-1 and S3-(3-5)	65
3.4.4	Synthesis of pyrazoline compounds from mono-chalcone	68
3.4.5	Synthesis of pyrimidine compounds from mono-chalcone	77
3.5	<i>In-vitro</i> assays	86
3.5.1	Cell viability assay	86
3.5.2	Recombinant EGFR kinase assay	87
<b>CHAPTER 4</b>	<b>RESULTS &amp; DISCUSSION</b>	<b>89</b>
4.1	Molecular Docking	89
4.1.1	Docking Score of mono- and tri-chalcone derivatives	89
4.1.2	Docking Score of pyrazoline derivatives	96

4.1.3	Docking Score of pyrimidine derivatives .....	100
4.2	Molecular Dynamic.....	105
4.2.1	Root Mean Square Deviation (RMSD).....	107
4.2.2	Hydrogen bonding analysis.....	109
4.2.3	Free energy of binding calculation .....	112
4.3	Spectral discussion of the synthesised compounds.....	114
4.3.1	Tri-chalcone compounds S1-1 and S1-2.....	114
4.3.2	Tri-chalcone compounds, S2-1 and S2-2.....	121
4.3.3	Synthesis of mono-chalcone S3-1 and S3-(3-5).....	125
4.3.4	Synthesis of pyrazoline derivatives S3-(Ai-Aiii) from mono chalcone .....	133
4.3.5	Synthesis of pyrimidine derivatives S3-(Bi-Biii) from mono chalcone .....	146
<b>CHAPTER 5 CYTOTOXICITY STUDY.....</b>		<b>158</b>
5.1	In-vitro assays for chalcone compounds .....	158
5.1.1	Cell viability assay .....	158
5.1.2	Recombinant EGFR kinase assay.....	161
5.2	In-vitro assays for pyrazoline and pyrimidine compounds .....	163
5.2.1	Cell viability assay .....	163
5.2.2	Recombinant EGFR kinase assay.....	166
<b>CHAPTER 6 CONCLUSION.....</b>		<b>167</b>
<b>REFERENCES .....</b>		<b>169</b>
<b>APPENDICES</b>		
<b>LIST OF PUBLICATIONS</b>		
<b>CONFERENCE</b>		



## LIST OF TABLES

	Page
Table 4.1	Free binding energies (FBE) of TAK-285 and 8 chalcone derivatives provided by AutoDock 4.2 and the interactive amino acids that formed H-bonds within the EGFR active site..... 91
Table 4.2	Free binding energies (FBE) of TAK-285 and the synthesised pyrazoline derivatives provided by AutoDock 4.2, and the interactive amino acids that formed H-bonds within the EGFR active site ..... 96
Table 4.3	Free binding energies (FBE) of TAK-285 and the synthesised pyrimidine derivatives provided by AutoDock 4.2, and the interactive amino acids that formed H-bonds within the EGFR active site ..... 101
Table 4.4	Hydrogen bonds analysis with MD simulation for the EGFR inhibitors within the ATP active site ..... 111
Table 4.5	Total binding energy and its components of TAK-285, <b>S1-1</b> and <b>S1-2</b> complexes obtained from MM-GBSA..... 113
Table 4.6	Summary of IR, <sup>1</sup> H and <sup>13</sup> C-NMR data of chalcones <b>S1-1</b> and <b>S1-2</b> ..... 119
Table 4.7	COSY and HSQC NMR data of compound <b>S1-1</b> . ..... 121
Table 4.8	Summary of IR, <sup>1</sup> H, and <sup>13</sup> C-NMR data of compounds <b>S2-1</b> and <b>S2-2</b> . ..... 124
Table 4.9	Summary of IR, <sup>1</sup> H, and <sup>13</sup> C-NMR data of compounds <b>S3-1</b> and <b>S3-(3-5)</b> ..... 129
Table 4.10	<sup>1</sup> H, COSY and HSQC NMR data of compound <b>S3-1</b> . ..... 132
Table 4.11	IR, <sup>1</sup> H and <sup>13</sup> C-NMR data of pyrazoline <b>S3-1A</b> and <b>S3-(3-5)A</b> for R <sub>2</sub> = <b>i</b> . ..... 138
Table 4.12	IR, <sup>1</sup> H and <sup>13</sup> C-NMR data of pyrazoline <b>S3-1A</b> and <b>S3-(3-5)A</b> for R <sub>2</sub> = <b>ii</b> . ..... 140
Table 4.13	IR, <sup>1</sup> H and <sup>13</sup> C-NMR data of pyrazoline <b>S3-1A</b> and <b>S3-(3-5)A</b> for R <sub>2</sub> = <b>iii</b> . ..... 142
Table 4.14	<sup>1</sup> H, COSY and HSQC NMR data of pyrazoline <b>S3-1Aiii</b> . ..... 145
Table 4.15	IR, <sup>1</sup> H and <sup>13</sup> C-NMR data of pyrimidines <b>S3-1B</b> & <b>S3-(3-5)B</b> for R <sub>2</sub> = <b>i</b> . ..... 150

Table 4.16	IR, $^1\text{H}$ and $^{13}\text{C}$ -NMR data of pyrimidines <b>S3-1B</b> & <b>S3-(3-5)B</b> for $\text{R}_2 = \text{ii}$ .....	152
Table 4.17	IR, $^1\text{H}$ and $^{13}\text{C}$ -NMR data of pyrimidines <b>S3-1B</b> & <b>S3-(3-5)B</b> for $\text{R}_2 = \text{iii}$ .....	154
Table 4.18	$^1\text{H}$ , COSY and HSQC NMR data of pyrimidine <b>S3-1Bii</b> .....	157
Table 5.1	Cytotoxic effects of <b>S1-1</b> , <b>S1-2</b> , <b>S2-1</b> , <b>S2-2</b> , <b>S3-1</b> , <b>S3-3</b> , <b>S3-4</b> and <b>S3-5</b> against breast cancer cell lines (MCF-7, MDA-MB-231) and one non-cancerous cell lines (MCF-10A).....	160
Table 5.2	Cytotoxic effects of pyrazoline and pyrimidine derivatives against two breast cancer cell lines (MCF-7 and MDA-MB-231) and non-cancerous cell lines (MCF-10A).....	164

## LIST OF FIGURES

	<b>Page</b>
Figure 1.1	Chalcone, pyrazoline and pyrimidine scaffolds..... 5
Figure 2.1	Important type of protein kinases (Gotink & Verheul, 2010)..... 10
Figure 2.2	Chalcone in <i>trans</i> and <i>cis</i> configurations..... 12
Figure 2.3	Some common reactions for chalcone synthesis (Sever et al., 2018)..... 13
Figure 2.4	Synthesis of chalcone by Claisen-Schmidt condensation..... 14
Figure 2.5	Synthesis of chalcone by Aldol condensation..... 14
Figure 2.6	Synthesis of chalcone by Suzuki reaction..... 15
Figure 2.7	Synthesis of chalcone by Heck reaction ..... 15
Figure 2.8	Synthesis of chalcone by microwave-assisted reaction ..... 16
Figure 2.9	Synthesis of chalcone by ultrasound irradiation reaction ..... 16
Figure 2.10	Synthesis of chalcone by solvent-free reaction ..... 17
Figure 2.11	Example of drugs with chalcone scaffold..... 18
Figure 2.12	Synthesis of quinolinyl chalcone compounds <b>14</b> ..... 18
Figure 2.13	Synthesis of retinoid-chalcone hybrids <b>15</b> ..... 19
Figure 2.14	Synthesis of indolyl chalcones <b>16</b> ..... 19
Figure 2.15	Synthesis of chalcone <b>17</b> ..... 20
Figure 2.16	Synthesis of <i>O</i> -allyl chalcones <b>18</b> ..... 20
Figure 2.17	Synthesis of chalcones <b>22</b> and flavanones <b>23</b> ..... 21
Figure 2.18	Synthesis of quinazolinone-chalcone derivatives <b>25</b> ..... 22
Figure 2.19	Synthesis of heterocyclic chalcones <b>26</b> ..... 23
Figure 2.20	Synthesis of heteroaryl chalcones <b>27</b> ..... 23
Figure 2.21	Synthesis of new chalcone <b>34</b> ..... 26
Figure 2.22	Synthesis of 4-amino-5-cinnamoylthiazoles derivatives <b>35</b> ..... 27
Figure 2.23	Ring closure reactions of chalcones. .... 28

Figure 2.24	Different types of pyrazolines with one endocyclic double bond .....	28
Figure 2.25	Synthesis of pyrazolines from $\alpha,\beta$ -unsaturated carboxylic acid esters .....	29
Figure 2.26	Synthesis of pyrazolines from $\alpha,\beta$ -unsaturated ketone.....	29
Figure 2.27	Synthesis of pyrazolines from chalcone derivatives .....	30
Figure 2.28	Synthesis of quinoline-based pyrazolines .....	32
Figure 2.29	Synthesis of 3,5-disubstituted pyrazolines.....	32
Figure 2.30	Synthesis of 2,4-disubstituted-1,3-thiazoles pyrazoline .....	33
Figure 2.31	Pyrimidine derivatives in a nucleic acid (thymine, cytosine and uracil) .....	37
Figure 2.32	Commercially available anticancer drugs with pyrimidine ring.....	38
Figure 2.33	Synthesis of pyrimidine from chalcone .....	38
Figure 2.34	Synthesis of uracil and thymine derivatives .....	39
Figure 2.35	Synthesis of pyrimidine <b>52</b> .....	39
Figure 2.36	Condensation of chalcone and guanidine nitrate.....	40
Figure 2.37	Synthesis of resin-bound pyrimidine <b>54</b> .....	40
Figure 2.38	Synthesis of coumarin linked pyrimidine derivative <b>71</b> .....	45
Figure 2.39	Computer-Aided Drug Design Approaches.....	47
Figure 2.40	Summary of the protein-ligand interactions.....	48
Figure 2.41	Process of SBDD.....	49
Figure 4.1	Inset is the superimposition of the TAK-285 crystal structure (red) and docked TAK-285 (yellow) with RMSD = 0.89 Å .....	89
Figure 4.2	Superposition of TAK-285 and the selected 8 chalcones derivatives into the binding pocket of EGFR. TAK-285 (yellow), <b>S1-1</b> (black), <b>S1-2</b> (cyan), <b>S2-1</b> (brown), <b>S2-2</b> (pink), <b>S3-1</b> (purple), <b>S3-3</b> (green), <b>S3-4</b> (blue) and <b>S3-5</b> (orange) .....	92

Figure 4.3	2D & 3D intermolecular interactions between docked chalcone compounds <b>S1-1</b> , <b>S1-2</b> , <b>S2-1</b> , <b>S2-2</b> , <b>S3-1</b> , <b>S3-3</b> , <b>S3-4</b> and <b>S3-5</b> with 3POZ.PDB. Green and Pink coloured amino acids represent their contribution in hydrogen bond and hydrophobic interactions, respectively .....	95
Figure 4.4	2D & 3D intermolecular interactions between docked pyrazoline compounds <b>S3-1A(i-iii)</b> and <b>S3-(3-5)A(i-iii)</b> with 3POZ.PDB .....	100
Figure 4.5	2D & 3D intermolecular interactions between docked pyrimidine compounds <b>S3-1B(i-iii)</b> and <b>S3-(3-5)B(i-iii)</b> with 3POZ.PDB .....	104
Figure 4.6	MD simulation: Temperature profile during 7 ns for the (a) TAK-285, (b) <b>S1-1</b> and (c) <b>S1-2</b> .....	106
Figure 4.7	MD simulation: Pressure profile during equilibration for the (a) TAK-285, (b) <b>S1-1</b> and (c) <b>S1-2</b> .....	106
Figure 4.8	MD simulation: Energy profile for the (a) TAK-285, (b) <b>S1-1</b> and (c) <b>S1-2</b> . Total energy (grey color), potential energy (red color), kinetic energy (green color) .....	107
Figure 4.9	Plot of RMSD vs. time graph for TAK-285 (red), <b>S1-1</b> (blue) and <b>S1-2</b> (gray).....	108
Figure 4.10	Plot of RMSD vs. time graph for 3POZ-TAK-285 (red), 3POZ- <b>S1-1</b> (blue) and 3POZ- <b>S1-2</b> (gray) .....	109
Figure 4.11	Stick representation of simulated compounds in the active site forming hydrogen bond (green dots) interactions with (A) compounds <b>S1-1</b> , (B) compound <b>S1-2</b> and (C) TAK-285 .....	112
Figure 4.12	Structure of compounds <b>S1-1</b> and <b>S1-2</b> .....	115
Figure 4.13	IR spectrum of chalcone <b>S1-1</b> .....	115
Figure 4.14	<sup>1</sup> H NMR spectrum of compound <b>S1-1</b> (500 MHz, CDCl <sub>3</sub> ).....	116
Figure 4.15	(a) <sup>13</sup> C NMR, (b) DEPT 90 and (c) DEPT135 spectra of compound <b>S1-1</b> .....	118
Figure 4.16	<sup>1</sup> H- <sup>1</sup> H COSY NMR spectrum of compound <b>S1-1</b> in CDCl <sub>3</sub> .....	120
Figure 4.17	<sup>1</sup> H- <sup>13</sup> C HSQC NMR spectrum of compound <b>S1-1</b> in CDCl <sub>3</sub> .....	120
Figure 4.18	Structure of compounds <b>S2-1</b> and <b>S2-2</b> .....	121
Figure 4.19	IR spectrum of compound <b>S2-1</b> .....	122

Figure 4.20	<sup>1</sup> H NMR spectrum of compound <b>S2-1</b> (500 MHz, CDCl <sub>3</sub> ).....	123
Figure 4.21	<sup>13</sup> C NMR spectrum of compound <b>S2-1</b> (125 MHz, CDCl <sub>3</sub> ).....	124
Figure 4.22	Structure of compounds <b>S3-1 and S3-(3-5)</b> . ....	125
Figure 4.23	IR spectrum of compound <b>S3-1</b> . ....	126
Figure 4.24	<sup>1</sup> H NMR spectrum of compound <b>S3-1</b> (500 MHz, CDCl <sub>3</sub> ).....	127
Figure 4.25	(a) <sup>13</sup> C NMR, (b) DEPT 90 and (c) DEPT135 spectra of compound <b>S3-1</b> . ....	128
Figure 4.26	<sup>1</sup> H- <sup>1</sup> H COSY NMR spectrum of compound <b>S3-1</b> .....	131
Figure 4.27	<sup>1</sup> H- <sup>13</sup> C HSQC NMR spectrum of compound <b>S3-1</b> . ....	132
Figure 4.28	Structures of pyrazoline compounds <b>S3-1A(i-iii)</b> and <b>S3-(3-5)A(i-iii)</b> .....	133
Figure 4.29	IR spectrum of pyrazoline <b>S3-1Aiii</b> . ....	134
Figure 4.30	<sup>1</sup> H NMR spectrum of pyrazoline <b>S3-1Aiii</b> . ....	135
Figure 4.31	(a) <sup>13</sup> C NMR, (b) DEPT 90 and (c) DEPT135 spectra of pyrazoline .....	137
Figure 4.32	<sup>1</sup> H- <sup>1</sup> H COSY NMR spectrum of pyrazoline <b>S3-1Aiii</b> .....	144
Figure 4.33	<sup>1</sup> H- <sup>13</sup> C HSQC NMR spectrum of pyrazoline <b>S3-1Aiii</b> . ....	145
Figure 4.34	Structures of pyrimidine compounds <b>S3-1B(i-iii)</b> and <b>S3-(3-5)B(i-iii)</b> .....	146
Figure 4.35	IR spectrum of pyrimidine <b>S3-1Bii</b> .....	147
Figure 4.36	<sup>1</sup> H NMR spectrum of pyrimidine <b>S3-1Bii</b> (500 MHz, DMSO-d <sub>6</sub> ).....	148
Figure 4.37	(a) <sup>13</sup> C NMR, (b) DEPT 90 and (c) DEPT135 spectra of pyrimidine <b>S3-1Bii</b> (125 MHz, DMSO-d <sub>6</sub> ) .....	149
Figure 4.38	<sup>1</sup> H- <sup>1</sup> H COSY NMR spectrum of pyrimidine <b>S3-1Bii</b> . ....	156
Figure 4.39	<sup>1</sup> H- <sup>13</sup> C HSQC NMR spectrum of pyrimidine <b>S3-1Bii</b> .....	157
Figure 5.1	Cytotoxic activity of chalcone derivatives at 72 h in the inhibition of MCF-7 and MDA-MB-231 cells based on MTT assay. Data are expressed as mean ± SEM of a representative experiment performed in triplicate (n=3). *Symbol above the bars indicate significant differences. The significance was considered at P< 0.0001 .....	161

Figure 5.2	Recombinant kinase activity measured using ADP-Glo™ for compounds <b>S1-1</b> and <b>S1-2</b> at three different concentrations (0, 0.19 and 50 μM) .....	162
Figure 5.3	Cytotoxic activity of pyrazoline and pyrimidine derivatives at 72 h in the inhibition of MCF-7 cell based on MTT assay. ....	165
Figure 5.4	Cytotoxic activity of pyrazoline and pyrimidine derivatives at 72 h in the inhibition of MDA-MB-231 cell based on MTT assay. ....	165
Figure 5.5	Recombinant kinase activity measured using ADP-Glo™ for compounds <b>S3-4Aiii</b> and <b>S3-5Bii</b> at three different concentrations (0, 0.19 and 50 μM) .....	166

## LIST OF SCHEMES

	<b>Page</b>
Scheme 3.1	Synthesis of three types of chalcone series ..... 60
Scheme 3.2	Synthesis of tri-chalcone <b>S1-1</b> and <b>S1-2</b> ..... 61
Scheme 3.3	Synthesis of tri-chalcone, <b>S2-1</b> and <b>S2-2</b> ..... 63
Scheme 3.4	Synthesis of mono-chalcone compounds, <b>S3-(1, 3-5)</b> ..... 66
Scheme 3.5	Synthesis of mono-pyrazoline compounds, <b>S3-(1,3-5)-A(i-iii)</b> ..... 69
Scheme 3.6	Synthesis of pyrimidine compounds, <b>S3-(1,3-5)-B(i-iii)</b> ..... 78



## LIST OF SYMBOLS AND ABBREVIATIONS

$\delta$	Chemical shifts
$\mu\text{M}$	micromolar
$^{13}\text{C}$ NMR	Carbon Nuclear Magnetic Resonance
$^1\text{H}$ NMR	Hydrogen Nuclear Magnetic Resonance
$\text{\AA}$	Angstrom
A498	renal cancer cell line
A549 & H460	human lung adenocarcinoma cell lines
$\text{Al}_2\text{O}_3$	aluminum oxide
$\text{Ba}(\text{OH})_2$	barium hydroxide
$^\circ\text{C}$	degree Celsius
Ca9-22, HSC-2, HSC-3, HSC-4, Cal-27 and KB	cancer cell carcinoma (OSCC) cell lines
CCD-19Lu	human lung fibroblast cell line
$\text{GI}_{50}$	growth inhibition
HeLa	cervical cancer cell line
HEP-2	liver cancer cell line
HepG2	hepatocellular cancer cell line
HT-29 & SW480	colorectal cancer cell lines
HT-29, COLO-205, HCT-116 & HCT-15	colon cancer cell lines
$\text{IC}_{50}$	The half maximal inhibitory concentration
IMR-32 & K-N-MC	neuroblastoma cancer cell lines
K	kelvin
$\text{K}_2\text{CO}_3$	potassium carbonate
K-562, RPMI-8226, SR, CCRF- CEM and MOLT-4	leukemia cancer cell lines

KF-Al <sub>2</sub> O <sub>3</sub>	potassium fluoride on alumina
Ki	inhibition constant
KOH	Potassium hydroxide
LN229	Glioblastoma cell
MCF-7, MDA-MB-231, CAL-51, T-47D and MDA-MB-468	Breast carcinoma cell lines
MDA-MB-435 & SK-MEL-5	melanoma cancer cell lines
MIA PaCa-2 & PANC-1	human pancreatic cancer cell lines
MKN-45	gastric cancer cell line
MTT	3-(4,5-dimethylthiazol-2-yl)-2,5 diphenyl tetrazolium bromide
NaOH	sodium hydroxide
NH <sub>2</sub> NH <sub>2</sub>	hydrazine hydrate
nM	nanomolar
ns	Nanosecond
ns	nanoseconds
OVCAR-4 & NCI/ADR-RES	ovarian cancer cell lines
OVCAR-5	ovarian cancer cell line
PC-3	prostate cancer cell line
PC3, DU145	human prostate cancer cell line
ps	picoseconds
S	entropy
SF-295	brain cancer cell line
T	temperature
U87MG	human glioblastoma cell line
<i>vitro</i>	Latin for “within the glass”
<i>vivo</i>	Latin for “within the living”
WRL-68	human normal liver cell line

$\Delta E_{\text{elec}}$	Coulomb electrostatic
$\Delta E_{\text{int}}$	internal energy
$\Delta E_{\text{MM}}$	describes the molecular mechanical (MM)energy change in the gas phase
$\Delta E_{\text{vdw}}$	Van der Waals interaction
$\Delta G_{\text{GB}}$	the electrostatic solvation energy
$\Delta G_{\text{solv}}$	solvation free energy
$\Delta H$	enthalpy
$\mu\text{g/mL}$	microgram/milliliter
Abs	Absorbance
ALA	Alanine
AMBER	Assisted Model Building with Energy Refinement
ARG	Arginine
ASN	Asparagine
ASP	Aspartate
ATP	adenosine triphosphate
CA IX	carbonic anhydrase-IX
CADD	Computer-Aided Drug Design
CDK	cyclin-dependent kinases
CHARMm	Chemistry at Harvard Macromolecular Mechanics
CHN	Carbon, hydrogen and nitrogen
CNS	central nervous system
CVFF	Consistent Valence Force Field
CYS	Cysteine
DEPT	Distortionless Enhancement by Polarization Transfer
DMSO	Dimethyl sulfoxide

DNA	deoxyribonucleic acid
EGFR	epidermal growth factor receptor
ER	estrogen receptor
FTIR	Fourier Transform Infra- Red
GAFF	General Amber force field
GLN	Glutamine
GLY	Glycine
GROMOS	Groningen Molecular Simulation package
HER	Human Epidermal Growth Factor Receptor
LBDD	Ligand-based drug design
LEU	Leucine
LGA	Lamarckian genetic algorithm
LYS	Lysine
MD	molecular dynamics
MET	Methionine
MWI	Microwave irradiation
PDB	Protein Data Base
PHE	Phenylalanine
ppm	Parts per million
QSAR	Quantitative Structure-Activity Relationship
RMSD	Root Mean Square Deviation
RNA	ribonucleic acid
ROS	reactive oxygen species
SBDD	Structure-based drug design
SER	Serine
STKs	serine-threonine kinases
THR	Threonine

TKs	tyrosine kinases
TLC	Thin layer chromatography
TMS	Tetramethylsilane
TYR	Tyrosine
US FDA	United States Food and Drug Administration
VAL	Valine
VEGFR	Vascular Endothelial Growth Factor Receptor

## LIST OF APPENDICES

- Appendix 1 (a) IR (b)  $^1\text{H}$  and (c)  $^{13}\text{C}$  NMR spectra of chalcone **S1-2** in  $\text{CDCl}_3$
- Appendix 2 (a) IR (b)  $^1\text{H}$  and (c)  $^{13}\text{C}$  NMR spectra of chalcone **S2-2** in  $\text{CDCl}_3$
- Appendix 3 (a) IR (b)  $^1\text{H}$  and (c)  $^{13}\text{C}$  NMR spectra of chalcone **S3-3** in  $\text{CDCl}_3$
- Appendix 4 (a) IR (b)  $^1\text{H}$  and (c)  $^{13}\text{C}$  NMR spectra of chalcone **S3-4** in  $\text{CDCl}_3$
- Appendix 5 (a) IR (b)  $^1\text{H}$  and (c)  $^{13}\text{C}$  NMR spectra of chalcone **S3-5** in  $\text{DMSO-d}_6$
- Appendix 6 (a) IR (b)  $^1\text{H}$  and (c)  $^{13}\text{C}$  NMR spectra of pyrazoline **S3-1Ai** in  $\text{DMSO-d}_6$
- Appendix 7 (a) IR (b)  $^1\text{H}$  and (c)  $^{13}\text{C}$  NMR spectra of pyrazoline **S3-3Ai** in  $\text{DMSO-d}_6$
- Appendix 8 (a) IR (b)  $^1\text{H}$  and (c)  $^{13}\text{C}$  NMR spectra of pyrazoline **S3-4Ai** in  $\text{DMSO-d}_6$
- Appendix 9 (a) IR (b)  $^1\text{H}$  and (c)  $^{13}\text{C}$  NMR spectra of pyrazoline **S3-5Ai** in  $\text{DMSO-d}_6$
- Appendix 10 (a) IR (b)  $^1\text{H}$  and (c)  $^{13}\text{C}$  NMR spectra of pyrazoline **S3-1Aii** in  $\text{DMSO-d}_6$
- Appendix 11 (a) IR (b)  $^1\text{H}$  and (c)  $^{13}\text{C}$  NMR spectra of pyrazoline **S3-3Aii** in  $\text{CDCl}_3$
- Appendix 12 (a) IR (b)  $^1\text{H}$  and (c)  $^{13}\text{C}$  NMR spectra of pyrazoline **S3-4Aii** in  $\text{CDCl}_3$
- Appendix 13 (a) IR (b)  $^1\text{H}$  and (c)  $^{13}\text{C}$  NMR spectra of pyrazoline **S3-5Aii** in  $\text{CDCl}_3$
- Appendix 14 (a) IR (b)  $^1\text{H}$  and (c)  $^{13}\text{C}$  NMR spectra of pyrazoline **S3-3Aiii** in  $\text{CDCl}_3$
- Appendix 15 (a) IR (b)  $^1\text{H}$  and (c)  $^{13}\text{C}$  NMR spectra of pyrazoline **S3-4Aiii** in  $\text{CDCl}_3$
- Appendix 16 (a) IR (b)  $^1\text{H}$  and (c)  $^{13}\text{C}$  NMR spectra of pyrazoline **S3-5Aiii** in  $\text{CDCl}_3$
- Appendix 17 (a) IR (b)  $^1\text{H}$  and (c)  $^{13}\text{C}$  NMR spectra of pyrimidine **S3-1Bi** in  $\text{DMSO-d}_6$

- Appendix 18 (a) IR (b)  $^1\text{H}$  and (c)  $^{13}\text{C}$  NMR spectra of pyrimidine **S3-3Bi** in DMSO- $\text{d}_6$
- Appendix 19 (a) IR (b)  $^1\text{H}$  and (c)  $^{13}\text{C}$  NMR spectra of pyrimidine **S3-4Bi** in DMSO- $\text{d}_6$
- Appendix 20 (a) IR (b)  $^1\text{H}$  and (c)  $^{13}\text{C}$  NMR spectra of pyrimidine **S3-5Bi** in DMSO- $\text{d}_6$
- Appendix 21 (a) IR (b)  $^1\text{H}$  and (c)  $^{13}\text{C}$  NMR spectra of pyrimidine **S3-3Bii** in DMSO- $\text{d}_6$
- Appendix 22 (a) IR (b)  $^1\text{H}$  and (c)  $^{13}\text{C}$  NMR spectra of pyrimidine **S3-4Bii** in DMSO- $\text{d}_6$
- Appendix 23 (a) IR (b)  $^1\text{H}$  and (c)  $^{13}\text{C}$  NMR spectra of pyrimidine **S3-5Bii** in DMSO- $\text{d}_6$
- Appendix 24 (a) IR (b)  $^1\text{H}$  and (c)  $^{13}\text{C}$  NMR spectra of pyrimidine **S3-1Biii** in DMSO- $\text{d}_6$
- Appendix 25 (a) IR (b)  $^1\text{H}$  and (c)  $^{13}\text{C}$  NMR spectra of pyrimidine **S3-3Biii** in DMSO- $\text{d}_6$
- Appendix 26 (a) IR (b)  $^1\text{H}$  and (c)  $^{13}\text{C}$  NMR spectra of pyrimidine **S3-4Biii** in DMSO- $\text{d}_6$
- Appendix 27 (a) IR (b)  $^1\text{H}$  and (c)  $^{13}\text{C}$  NMR spectra of pyrimidine **S3-5Biii** in DMSO- $\text{d}_6$

**PERMODELAN MOLEKUL, SINTESIS, PENCIRIAN DAN AKTIVITI  
SITOTOKSIK TERBITAN BAHARU KALKON, PIRAZOLINA DAN  
PIRIMIDINA**

**ABSTRAK**

Tiga siri baharu terbitan kalkon yang mempunyai aktiviti antikanser yang baik telah dikaji iaitu dua siri terbitan tri-kalkon **S1(1-7)** dan **S2(1-7)**, dan satu terbitan mono-kalkon **S3(1-7)**. Tiga siri lain pirazolina **Ai-Aiii** dan pirimidina **Bi-Biii** daripada mono-kalkon juga telah dikaji menggunakan AutoDock 4.2.6. Interaksi antara molekul dan tenaga pengikatan bagi sebatian yang dicadangkan telah dikenalpasti untuk disintesis dan dicirikan. Sebatian yang terbaik telah dipilih untuk analisa lebih lanjut secara simulasi MD menggunakan AMBER 14. Sebatian berikut yang terdiri daripada terbitan kalkon, **S1-1, S1-2, S2-1, S2-2, S3-1, S3-(3-5)**, terbitan pirazolina, **Ai-Aiii** dan pirimidina, **Bi-Biii** daripada mono-kalkon **S3-(1,3-5)** menunjukkan afiniti pengikatan yang tinggi bagi interaksi dengan tapak pengikatan aktif EGFR. Semua terbitan kalkon, pirazolina dan pirimidina yang dipilih ini telah disintesis untuk ujian aktiviti sitotoksik terhadap sel kanser payudara dan aktiviti perencatan EGFR. Sintesis terbitan kalkon telah dijalankan secara kondensasi Claisen-Schmidt manakala penutupan gelang bagi mono-kalkon telah membentuk terbitan pirazolina dan pirimidina. Struktur kimia bagi sebatian yang disintesis telah ditentukan melalui teknik spektroskopi seperti FTIR, <sup>1</sup>H NMR, <sup>13</sup>C NMR dan analisa unsur CHN. Aktiviti antiproliferatif bagi sebatian yang disintesis terhadap sel kanser payudara (MCF-7 dan MDA-MB-231) telah ditentukan secara ujian 3-(4,5-dimetiltiazol-2-il)-2,5-difeniltetrazolium bromida (MTT). Aktiviti perencatan faktor pertumbuhan epidermis bagi sebatian yang paling sitotoksik telah dinilai menggunakan ujian Kinase ADP-



Glo™ (Promega, Madison). Yang menariknya, sebatian **S1-1** dan **S1-2** menunjukkan aktiviti antiproliferatif yang kuat bagi MCF-7 ( $2.23 \pm 0.11$  dan  $2.04 \pm 0.01$   $\mu\text{M}$ ) serta MDA-MB-231 ( $6.44 \pm 0.11$  dan  $3.75 \pm 0.26$   $\mu\text{M}$ ), relatif kepada tamoksifen dengan  $\text{IC}_{50}$  masing-masing sebagai  $9.3 \pm 0.44$  dan  $18.92 \pm 1.43$   $\mu\text{M}$ . Analisa ikatan hidrogen yang menyeluruh sepanjang simulasi dinamik molekul 7 ns bagi sebatian **S1-1** dan **S1-2** telah menunjukkan kemampuan sebatian ini untuk mengekalkan interaksi yang diperlukan bagi perencatan, terutamanya interaksi dengan MET 793 dan LYS 745. Pengiraan MM-GBSA menunjukkan bahawa ligan membentuk ikatan yang kuat dalam tapak aktif, dengan tenaga pengikatan  $-56.6$  dan  $-44.04$  kcal/mol bagi sebatian **S1-1** and **S1-2**, masing-masing. Tenaga pengikatan ini adalah setara dengan TAK-285 ( $-66.17$  kcal/mol), yang menunjukkan bahawa sebatian **S1-1** dan **S1-2** menunjukkan peningkatan yang ketara dalam rawatan ketahanan antikanser. Ini disebabkan oleh kesan yang berpotensi terhadap EGFR sebagai perencat yang diramalkan oleh kajian simulasi dinamik molekul dan analisa EGFR secara *in vitro*. Kesan anti-ER yang mungkin telah diramalkan oleh kajian secara *in vitro*.

**MOLECULAR MODELLING, SYNTHESIS, CHARACTERISATION AND  
CYTOTOXICITY ACTIVITY OF NEW CHALCONE, PYRAZOLINE AND  
PYRIMIDINE DERIVATIVES**

**ABSTRACT**

Three new series of novel chalcone derivatives with promising anti-cancer activity were studied which are two series of tri-chalcone derivatives **S1(1-7)** and **S2(1-7)** and a series of mono-chalcone derivatives **S3(1-7)**. Another three series of pyrazoline **Ai-Aiii** and pyrimidine **Bi-Biii** from mono-chalcone were also studied by AutoDock 4.2.6. The intermolecular interactions and binding energies of the proposed compounds were determined to be synthesised and characterized. The best compounds were selected for further investigation by MD simulation using AMBER 14. The following compounds of chalcone derivatives **S1-1, S1-2, S2-1, S2-2, S3-1, S3-(3-5)**, pyrazoline derivatives **Ai-Aiii** and pyrimidine **Bi-Biii** from mono-chalcone **S3-(1,3-5)** demonstrated the highest binding affinity for the interaction with the active EGFR binding site. These selected chalcones, pyrazoline and pyrimidine derivatives were synthesised to test their cytotoxicity activity against breast cancer cell lines and EGFR inhibitory activity. Synthesis of the chalcone derivatives was performed via a Claisen-Schmidt condensation while the ring-closing of mono-chalcones formed the pyrazoline and pyrimidine derivatives. The chemical structures of the synthesised compounds were confirmed using spectroscopic techniques such as FTIR, <sup>1</sup>H NMR, <sup>13</sup>C NMR and elemental analysis (CHN analysis). Antiproliferative activity of the synthesised compounds against breast cancer cell lines (MCF-7 and MDA-MB-231) were evaluated using 3-(4,5-dimethylthiazole-2-yl)-2,5-diphenyltetrazolium bromide assay (MTT). The epidermal growth factor inhibition activity of the most cytotoxic

compounds was assessed using ADP-Glo™ Kinase Assay (Promega, Madison). Interestingly, compounds **S1-1** and **S1-2** showed potent antiproliferative activity of MCF-7 ( $2.23 \pm 0.11$  and  $2.04 \pm 0.71$   $\mu\text{M}$ ) and MDA-MB-231 ( $6.44 \pm 0.01$  and  $3.75 \pm 0.26$   $\mu\text{M}$ ), relative to tamoxifen  $\text{IC}_{50}$  of  $9.3 \pm 0.44$  and  $18.92 \pm 1.43$   $\mu\text{M}$ , respectively. Extensive hydrogen bond analysis throughout 7 ns molecular dynamics simulation of compounds **S1-1** and **S1-2** demonstrated the capacity of these compounds to retain the interactions that exert the inhibitory effect, especially interactions with MET 793 and LYS 745. The MM-GBSA calculations illustrated that the ligands form a powerful bond within the target site with binding energies of -56.6 and -44.04 kcal/mol for compounds **S1-1** and **S1-2**, respectively. These binding energies were comparable with TAK-285 (-66.17 kcal/mol), which indicated that compounds **S1-1** and **S1-2** showed a significant improvement in the anticancer resistant treatment. This is due to their potential effects on the EGFR as inhibitors which were predicted by molecular dynamics simulation studies and *in-vitro* EGFR analysis. Their possible anti-ER effect was predicted by the *in-vitro* studies.

## CHAPTER 1

### INTRODUCTION

#### 1.1 Background of the study

##### 1.1.1 Cancer

Cancer is a group of diseases with abnormal cell growth that can spread into or invade nearby tissues. Cancer arises due to the transformation of a normal cell into a tumour cell, progressing from a lump to a malignant tumour. Such transformation is due to the low capability of the normal cells to neutralise the production of excess free radicals in the surrounding, causing the cells to grow out of control in an irregular way (Cooper, 2000). Cancer remains a major global health problem, affecting both developed and developing countries and has also been reported as the second-highest cause of death after cardiovascular diseases. According to the 2014 World Health Organization report, breast cancer is one of the most common cancer, diagnosed in women and a major cause of death worldwide (Fitzmaurice et al., 2017).

There are many types of cancer treatment, depending on the type of cancer and stages of diagnosis. Some cancer patients need only one treatment while others need a combination of treatments, such as surgery with chemotherapy and/or radiation therapy (Nowecki & Jeziorski, 2017). Other treatments include immunotherapy, targeted therapy or hormone therapy (Coates et al., 2015; Vanderpuye et al., 2017). If cancer has not spread into the surrounding tissues, surgery and radiotherapy can remove the tumour. If the cancer cells have spread, systemic treatment such as chemotherapy is needed which involves the use of agents that act by inhibiting cell division in cancerous cells and ultimately destroying them.

The use of chemotherapeutic agents has been associated with the reduction of the mortality rate (Perazella, 2012; Thavendiranathan et al., 2013; Dasari &

Tchounwou, 2014; Zhang et al., 2018). However, these chemotherapeutic agents lead to adverse effects as a result of damage to normal body cells and organ toxicities which reduced the quality of life in cancer patients (Eckhardt, 2002; Skrzydlewska et al., 2005; Varmus, 2006; Hassan et al., 2016). On balance, these chemotherapeutic agents cannot differentiate between the two types of cells (Tang et al., 2017). Such effects include hand-foot syndrome, neuropathy, allergic reactions, diarrhea, mouth sores, loss of appetite, nausea, vomiting, easy bleeding which increase infections, fatigue (Sommariva et al., 2016), chronic kidney disease (Perazella, 2012), cardiac injury, heart failure and liver damage (Dasari & Tchounwou, 2014), dermatological toxicities such as hair loss, skin and nail damage (Sibaud et al., 2016). Another major problem is the resistance of the cancer cells to the drugs, leading to the failure of treatment and also complications including relapse, metastasis and death (Hassan et al., 2016; Housman et al., 2014; Tang et al., 2017; Zhang et al., 2018).

Chemo-resistance (resistance to chemotherapy) has emerged as a major problem in breast cancer. Acquired resistance can reverse the initial reduction of tumour size. This causes disease progression and conferring resistance to other chemotherapeutic agents with different structures and mechanisms of action, a phenomenon known as multidrug resistance (Tang et al., 2017). Several strategies have been used to overcome chemo-resistance in breast cancer including combination therapy, immunotherapy, gene therapy, and novel drug delivery. Although their effects are not satisfactory due to toxicity, and drug-drug interactions (Ji et al., 2019), the use of chemotherapeutic agents has shown improvement in the survival of cancer patients (Thavendiranathan et al., 2013; Zhang et al., 2018). The problem of chemo-resistance coupled with the high adverse effect has shifted the sight of the research community to design new agents that have minimal side effects, can overcome the challenge of

resistance, and can target tyrosine kinase sub-proteins such as Epidermal Growth Factor Receptors (EGFRs) (Ji et al., 2019).

### **1.1.2 Epidermal Growth Factor Receptors (EGFRs)**

Strong EGFR expression in breast cancer has been investigated by several studies, especially in tamoxifen-resistant breast cancer cases (Massarweh et al., 2008; Li et al., 2013; Huang & Fu, 2015). Since targeting the estrogen receptor is not a unique survival track for breast tumours, the EGFR pathway offers the alternative. The positive breast tumours of the estrogen receptor (ER- $\alpha$ ) that initially possess low or normal levels of EGFR usually gain drastically over-expressed EGFR during the development of the tamoxifen resistance (Li et al., 2013; Sharma et al., 2019). Thus, the combined treatment of the EGFR inhibitor with tamoxifen has demonstrated an improvement in the sensitivity of cancerous cells toward the tamoxifen (Gee et al., 2003).

EGFR acts as a significant growth signal receptor that regulates cell division and survival (Mok et al., 2014). It is considered as the source of stimulus for cancer cell proliferation. There is a strong correlation between the overexpression, amplification and mutation of these proteins with cancers; particularly breast cancers (Wykosky et al., 2011; Huang & Fu, 2015). Auto-phosphorylation of EGFR is a crucial step that triggers many pathways involved in the cellular division (Jotte & Spiegel, 2015). This EGFR pathway plays a significant role in carcinogenesis, progression and metastasis of cancer, and it is currently targeted by numerous chemotherapeutic agents (Chen, 2013; Goffin & Zbuk, 2013). Such agents include small molecule inhibitors such as chalcones in the management of cancer including breast cancer (Ji et al., 2019). The use of these small molecule inhibitors is encouraged by their unique structures

which leads to significant affinities and activities of targeting cancer cells (Elkhalifa et al., 2019).

### **1.1.3 Chalcones, pyrazoline and pyrimidine scaffold as anticancer agent**

Chalcones ( $\alpha,\beta$ -unsaturated ketones) represent one of the largest classes of plant metabolites which is a flavonoid. It is one of the natural products that has existed as a core structure of several drugs such as EGFR inhibitors in the development of anticancer agents (Youssef et al., 2004; Manojkumar et al., 2009; Lee et al., 2011; Bayomi et al., 2013; Xu et al., 2013; Bayomi et al., 2015; Starok et al., 2015; Wada et al., 2015; Qin et al., 2017). Chalcone possesses anti-EGFR kinase activity owing to its high hydrogen bonding and hydrophobic interactions which can inhibit the proliferation of cancer cells (Yang et al., 2001, Ji et al., 2013). Chalcones remain to be the attractive scaffolds due to their abundance in plants and easy synthesis methods. It has the structure of two aromatic rings joined by the  $\alpha,\beta$ -unsaturated system (Sapra et al., 2016), as shown in Figure 1.1. Chalcone is a well-known intermediate that can be used to synthesise different types of heterocyclic compounds.

Heterocyclic scaffolds can be found in a wide variety of drugs and many biologically active compounds of natural products. It was reported that compounds with the nitrogen heterocyclic scaffold, in particular, pyrazoline and pyrimidine exhibited several pharmacological properties and have become important in the development of new effective drugs for cancer. Nitrogen-based heterocyclic compounds makeup nearly 60% of all drugs approved by the FDA (Vitaku et al., 2014) and represent about 73% of the approved anticancer drugs in 2015 (Hosseinzadeh et al., 2018). Pyrazoline, which is a five-membered heterocyclic ring containing two adjacent nitrogen atoms (Figure 1.1) is among the most prominent heterocyclic

compounds with a wide spectrum of biological activities (Arora et al., 2012). Pyrimidine, on the other hand, is a 6-membered heterocyclic unit containing two nitrogen atoms (Figure 1.1) have been reported to have wide application, especially as anticancer agents (Arora et al., 2012; Sliwoski et al., 2014; James et al., 2017; Yunta, 2017; Özdemir et al., 2018; Sever et al., 2018 ). In the last decade, substituted pyrimidine ring systems, have also been reported as EGFR-kinase inhibitors and anticancer agents ( Traxler et al., 1996; Traxler et al., 2001; Thirumurugan et al., 2018).

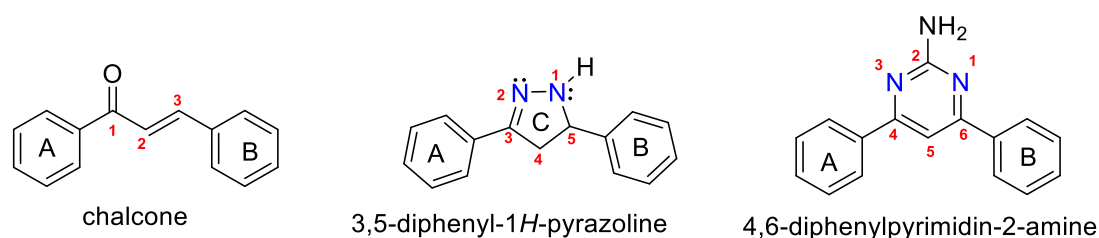


Figure 1.1: Chalcone, pyrazoline and pyrimidine scaffolds

Recently, the presence of multi-structural units, or polyvalent, bound to a central core may cause simultaneous interactions with multiple receptors (Burmaoglu et al., 2019) has become a preferred route for the design of active agents that might be novel drug candidates. Compared to the monovalent, polyvalent interactions are much stronger and provide the basis for mechanisms of both agonizing and antagonizing biological interactions which are fundamentally different from those in monovalent systems (Chooi, 2004; Vance et al., 2008).

## 1.2 Problem Statement

Since chemotherapeutic drugs cannot differentiate between cancer and normal cells (Tang et al., 2017), there is a need to continuously develop new drugs that are more efficient in targeting the tumour cells and safe to the normal cells. The



development of new chemotherapeutic agents will be more selective to produce drugs with fewer side effects ( El-Azab et al., 2010; Alaa et al., 2012; Alanazi et al., 2013; Al-Suwaidan et al., 2013; Alanazi et al., 2014; Abdel-Aziz et al., 2016; Al-Suwaidan et al., 2016; Alanazi et al., 2016; Mohamed, et al., 2016). Another problem with chemotherapy drugs in cancer treatment is the restricted effectiveness due to drug resistance which targeted the tyrosine kinase sub-proteins such as Epidermal Growth Factor Receptor (EGFR) (Ji et al., 2019). EGFR is found on the surface of normal cells that are involved in cell growth when an epidermal growth factor binds to it. EGFR is also found at high levels on some types of cancer cells. EGFR inhibitors such as ErbB-1 or HER-1 inhibitors are used to block these cancer cells to grow and divide. Several studies have investigated the EGFR expression in breast cancer. However, limited findings in the discovery of new anticancer agents targeting the Epidermal Growth Factor Receptor have initiated this work.

Tri-chalcone derivatives with multi-structural units, causing simultaneous interactions with multiple receptors have become the preferred targets for the design of new molecules. Notably, in the last decade, few tris-chalcone compounds have been reported as versatile precursors for medical and industrial applications (Sum et al., 2017; Mahmoodi & Zeydi, 2018). Recently, nitrogen-based heterocycles are considered a unique scaffold for various drugs because they exhibited a wide range of enhanced biological activities. Based on the above-mentioned criteria, this work focused on the synthesis of some chosen compounds of the tris- and mono-chalcone derivatives, their computational docking and molecular dynamics (MD) techniques to examine these new compounds with chalcone, pyrazoline and pyrimidine scaffolds as potential EGFR inhibitors and as anticancer agents against various cancer cell lines. Moreover, the evaluation of their *in-vitro* cytotoxic activity against cancerous and non-

cancerous cell lines of breast cells has also been determined. The EGFR kinase inhibitory assay of the compounds that possess the highest antiproliferative activity against breast cancer cell lines has also been tested to confirm the multitarget cytotoxic effect.

### **1.3 Objectives**

The objectives of this work include:

1. To design the active molecules using molecular docking and molecular dynamics (MD) techniques.
2. To synthesise and characterise two series of tris-chalcone and a series of mono-chalcone derivatives via a Claisen-Schmidt condensation reaction.
3. To synthesise and characterise different series of heterocyclic derivatives with pyrazoline and pyrimidine scaffolds.
4. To evaluate the *in vitro* cytotoxic activities and EGFR activities of the synthesised compounds against the breast cancer cell lines (MCF-7 and MDA-MB-231).

#### **1.4 The scope of the study**

The molecular dynamic work was done at the Molecular Modeling and Drug Design Lab, Department of Pharmaceutical Sciences, Faculty of Pharmacy, Al-Ahliyya Amman University, Amman, Jordan, under the supervision of the field supervisor, Dr. Belal O. Al-Najjar. All the synthesised compounds were characterised using the instruments located at the School of Chemical Sciences, Universiti Sains Malaysia. The selected compounds were sent to the Advanced Medical and Dental Institute, USM in Bertam for cytotoxicity assays under the supervision of Dr Nik Nur Syazni Nik Mohamed Kamal. Finally, the *in vitro* enzymatic assay was done in Al-Ahliyya Amman University under the supervision of Dr Belal Al-Najjar.

## CHAPTER 2

### LITERATURE REVIEW

#### 2.1 Tyrosine kinase protein-inhibitors

One of the most important targets is protein tyrosine kinase (PTK) inhibitor which plays an important role in the signal transduction process, leading to cell proliferation, differentiation, migration, metabolism and programmed cell death. Protein kinases are divided based on amino acids. Tyrosine kinases (TKs) phosphorylates the phenolic hydroxyl group of tyrosine residues while serine-threonine kinases (STKs) phosphorylates the alcohol group of serine and threonine residues, as shown in Figure 2.1 (Gotink & Verheul, 2010). The signaling pathways involved in cancer initiation and progression rely on the activity of kinase enzymes which act as important co-factors in signal transduction. (Collins & Workman, 2006). These enzymes transfer the phosphate groups onto specific amino acid residues such as tyrosine, serine or threonine within protein kinases.

The tyrosine kinase protein-inhibitors are of great interest due to their capacity as therapeutic agents to treat a variety of diseases, especially cancer (Gschwind et al., 2004; Backes et al., 2008a; 2008b). Among the protein tyrosine kinase, the epidermal growth factor receptor (EGFR) has emerged as a key and main target for the development of new anticancer agents (Speake et al., 2005; Warnault et al., 2013; Yewale et al., 2013). EGFR kinase inhibition in cancer treatment is performed by blocking this enzyme with small molecules (drugs). To date, over 10 EGFR inhibitors have been approved by the United States Food and Drug Administration (US FDA) in the past two decades (Dowell et al., 2005). This includes Gefitinib, Lapatinib and Erlotinib (Stamos et al., 2002; Dowell et al., 2005; Ganjoo & Wakelee, 2007)

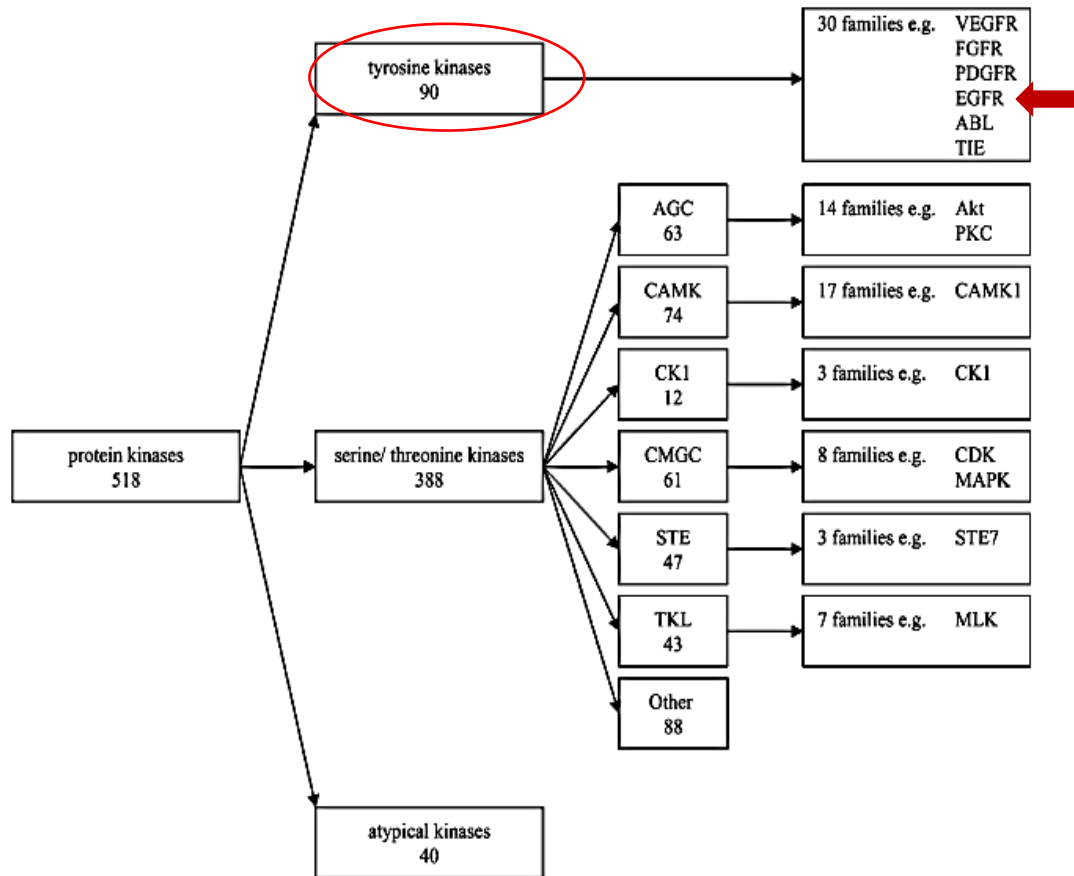
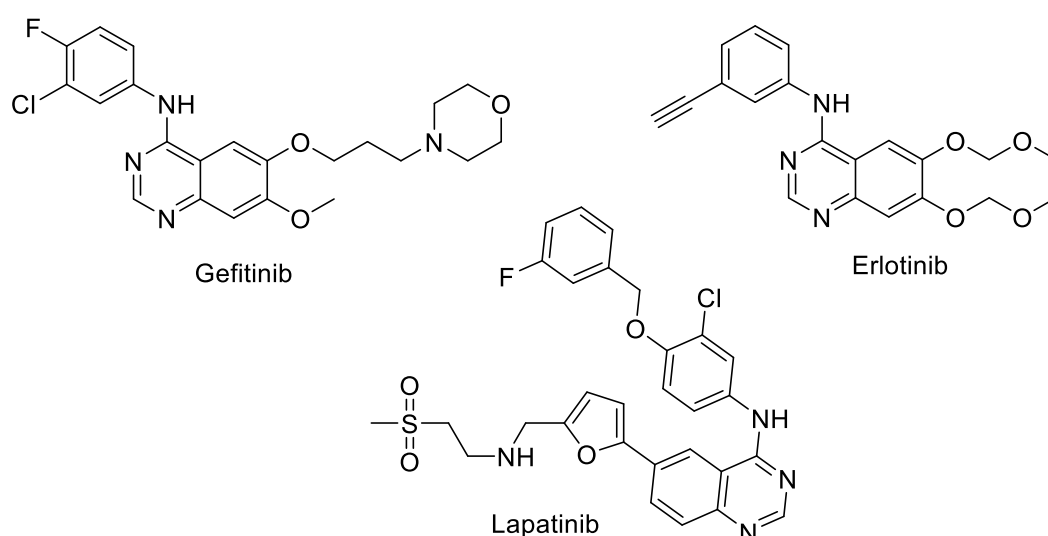


Figure 2.1: Important type of protein kinases (Gotink & Verheul, 2010)

Epidermal Growth Factor Receptor (EGFR) is a *transmembrane* polypeptide protein that belongs to the tyrosine kinase family. EGFRs can be classified into four categories, namely HER1 (ErbB-1), HER2 (ErbB-2), HER3 (ErbB-3), and HER4 (ErbB-4). They control the intracellular signal transduction pathways and are involved in the growth factor signaling which is important in tumour cell survival. Abnormal signaling of these factors leads to uncontrolled cell proliferation, inhibition of apoptosis, angiogenesis, migration, and metastasis of cancer cells (Feitelson et al., 2015). EGFR is found at high levels in cancer cells. Among the protein tyrosine kinases, EGFR has become a target for the development of anticancer agents (Ibrahim et al., 2012; Prashar et al., 2012). A variety of small molecule kinase inhibitors have been developed to target EGFR family members. Some of the molecules which inhibit

EGFR are effective in the treatment of cancer (Steelman et al., 2016). Gefitinib and Erlotinib are EGFR inhibitors which interrupt signals in the target cells. Lapatinib is a dual tyrosine kinase inhibitor that interrupts the HER2/neu and EGFR pathways that are used in the treatment of breast and lung cancer. Extensive researches have been done on the EGFR inhibitors. Several agents that inhibit individual ErbB receptors and the development of multiple ErbB inhibitors have been approved for the treatment of cancer validating ErbB receptors as therapeutic targets.



## 2.2 Chalcone as therapeutic agents

Most pharmaceutical drugs for cancer treatment have a unique moiety such as chalcone with various biological activities. Chalcone is a precursor of flavonoids and isoflavonoids in the plant kingdom, representing the secondary metabolites, a naturally occurring compound of the terrestrial plants (Bohm, 1998; Sahu et al., 2012). Chalcone compounds have various biological activities including anti-infectious (Prashar et al., 2012), anti-malarial (Domínguez et al., 2013), anticancer and antioxidative properties (Shaik et al., 2020), anti-inflammatory (Israf et al., 2007) anti-obesity (Birari et al., 2011) and anti-spasmodic potential (Sato et al., 2007). Chalcone, 1,3-diphenyl-2-propene-1-one contains a conjugated double bond that is connected by an  $\alpha,\beta$ -

unsaturated enone bridge (Kumar et al., 2013; Sapra et al., 2016). Chalcone adopts the *cis* or *trans* configurations (Figure 2.2) with the *trans* isomer being more stable and predominant while the *cis* isomer is unstable due to steric effects between the carbonyl group and the A-ring (Aksöz & Ertan, 2011). The  $\alpha,\beta$ -unsaturated carbonyl moiety in chalcone is capable to form irreversible bonds with biological macromolecules and hence resulted in toxic effects such as allergy, carcinogenicity and mutagenicity (Schwöbel et al., 2010). Such reactivity might be affected by the substituted pattern of the aromatic rings and the substituent of the double bond of the enone system (Amslinger et al., 2013).

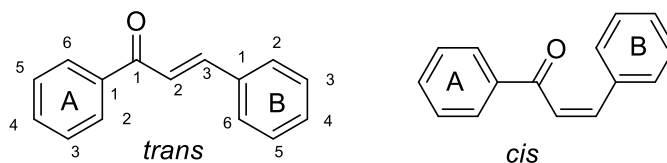


Figure 2.2: Chalcone in *trans* and *cis* configurations

Chalcones are promising targets to be used in several cancers including breast cancer because of their unique structure and significant affinity for cancer cells (Elkhalifa et al., 2019). Many natural and synthetic chalcones have demonstrated activity against cancer cells owing to their ability to act and inhibit several cancer targets (Mahapatra et al., 2015). Therefore, the understanding of the structure, molecular targets and structure-activity relationship could be used to design and develop new chalcone derivatives with good chemotherapeutic profiles that give minimal adverse effect and low cost (Mahapatra et al., 2015).

### 2.2.1 Synthesis of chalcone molecules

Chalcones are prepared by condensation reactions via base or acid catalysis using various routes (Özdemir et al., 2018; Sever et al., 2018). A growing number of new procedures for chalcones synthesis have been reported because of the development of different catalysts or reaction conditions. Various synthetic pathways of chalcones that have been reported are summarised in Figure 2.3.

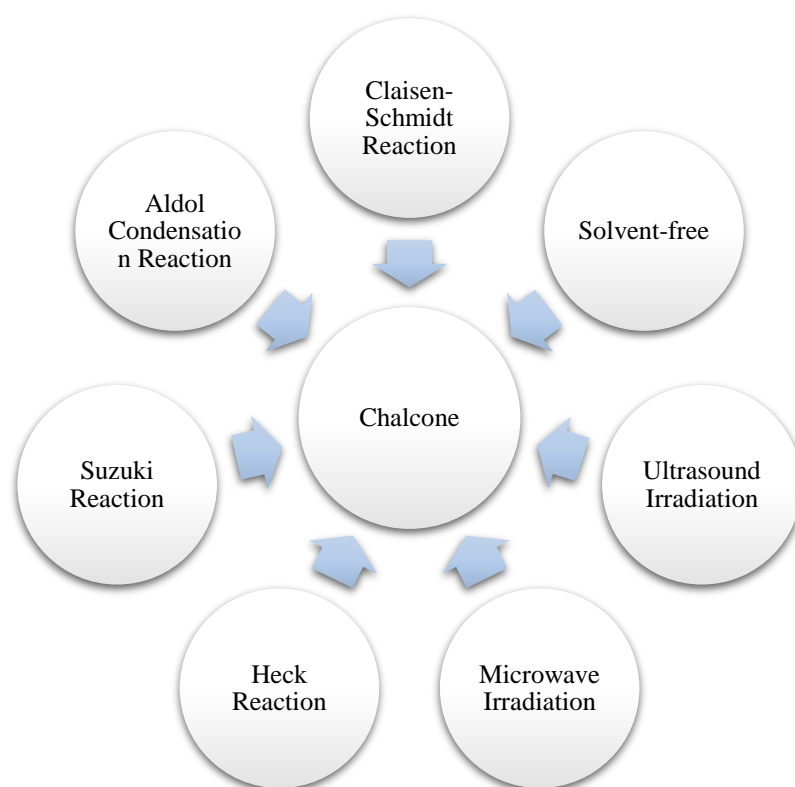


Figure 2.3: Some common reactions for chalcone synthesis (Sever et al., 2018)

#### 2.2.1(a) Claisen-Schmidt Condensation

The Claisen-Schmidt condensation involves a reaction of an equimolar quantity of substituted acetophenone and substituted benzaldehyde which is condensed in the presence of aqueous-alcoholic alkaline, as shown in Figure 2.4 (Mandge et al.,



2007). A 10% - 60% concentration of alkali is required and the reaction takes place at a temperature of 50°C for 12-15 hrs or at room temperature.

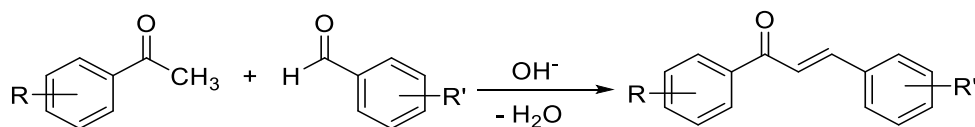


Figure 2.4: Synthesis of chalcone by Claisen-Schmidt condensation

### 2.2.1(b) Aldol Condensation

Aldol condensation involves a reaction between acetophenone and benzaldehyde (Figure 2.5). Acetophenone is treated with a base such as KOH or NaOH, and produced a product (intermediate) after reacting with benzaldehyde. The intermediate is heated to produce chalcone after losing one water molecule (Mukaiyama, 1982; Palaniandavar & Natarajan, 1980).

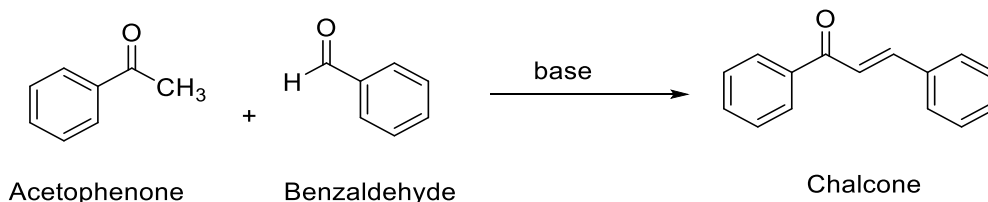


Figure 2.5: Synthesis of chalcone by Aldol condensation

### 2.2.1(c) Suzuki Reaction

The Suzuki reaction involves phenylboronic acid (1) and cinnamyl chloride (2) or other benzoyl chlorides (3) and phenyl vinyl boronic acid (4), as shown in Figure 2.6 (Eddarir et al., 2003).

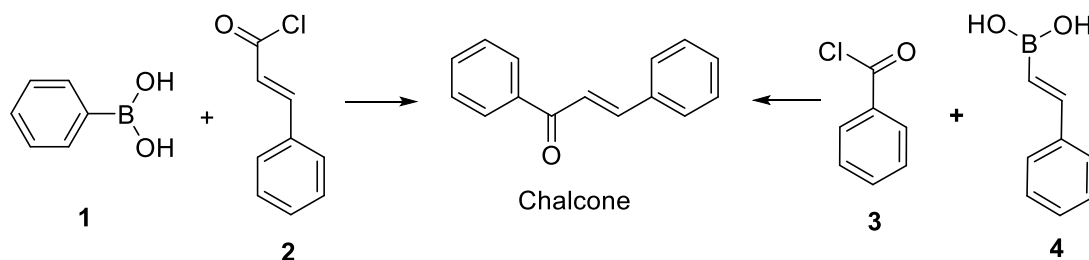


Figure 2.6: Synthesis of chalcone by Suzuki reaction

### 2.2.1(d) Heck Reaction

When an aryl vinyl ketone is combined with an aryl iodide under Heck reaction conditions, chalcones and other flavonoids are produced, as shown in Figure 2.7 (Bianco et al., 2003; Zou et al., 2007).

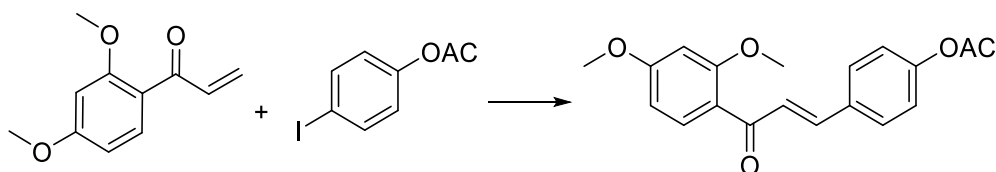
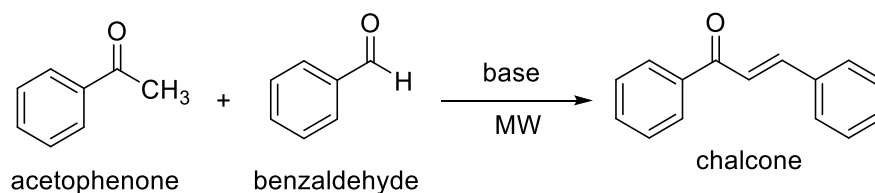


Figure 2.7: Synthesis of chalcone by Heck reaction

### 2.2.1(e) Reaction via Microwave Irradiation

Microwave irradiation is an important tool for green chemistry that dramatically reduces the reaction time, increases the yield and enhances product purities by reducing unwanted side reactions compared to conventional heating methods. In the preparation of chalcones and their analogs using microwave technique (Figure 2.8), heterogeneous and homogeneous catalysts such as potassium carbonate, barium hydroxide,  $\text{KF-Al}_2\text{O}_3$ , *p*-toluenesulfonic acid, zirconium tetrachloride, piperidine and aqueous alkali have been used (Gall et al., 1999; Blass, 2002; Bora et al., 2005).



base: NaOH (40%); CaO; K<sub>2</sub>CO<sub>3</sub>; NH<sub>4</sub>OH; TiO<sub>2</sub>SO<sub>4</sub>; clay

Figure 2.8: Synthesis of chalcone by microwave-assisted reaction

### 2.2.1(f) Reaction via Ultrasound Irradiation

Ultrasound irradiation has been employed in organic synthesis to accelerate and enhance the performance of the reaction. Compared to the conventional method, ultrasonic irradiation is a green synthetic technique in chemical reactions. Chalcones and their derivatives can be synthesized through ultrasound irradiation using heterogeneous and homogeneous catalysts such as potassium carbonate, basic Al<sub>2</sub>O<sub>3</sub>, amino-grafted zeolite, Ba(OH)<sub>2</sub>, pulverized KOH and KF-Al<sub>2</sub>O<sub>3</sub> (Fuentes et al., 1987; Wei et al., 2005; Calvino et al., 2006).

Younis and co-workers (2016) reported that the reaction of substituted acetophenone (**5**) with acetic acid under ultrasonic activation to form (**6**) which react with a series of aldehydes (**7**) in water as a benign medium to form (**8**) with improved yield and reaction time (Figure 2.9).

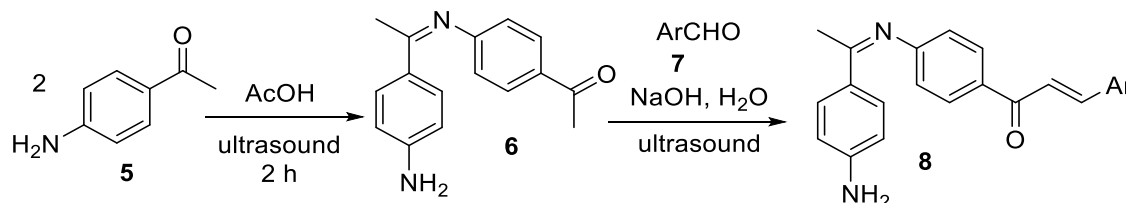


Figure 2.9: Synthesis of chalcone by ultrasound irradiation reaction

### 2.2.1(g) Reaction via solvent-free reaction

Rothenberg and colleagues (2001) posited that solid-solid reactions take place when a liquid melt is produced and this could be a eutectic mixture from mixed reactants. A high concentration of reactants in this solvent-free reaction increased the reaction rate. In Figure 2.10, benzaldehyde and acetophenone were mixed and melted before adding the base (NaOH). This results in the formation of a pasty mixture as the solid product of chalcone is produced and separated from the solution.

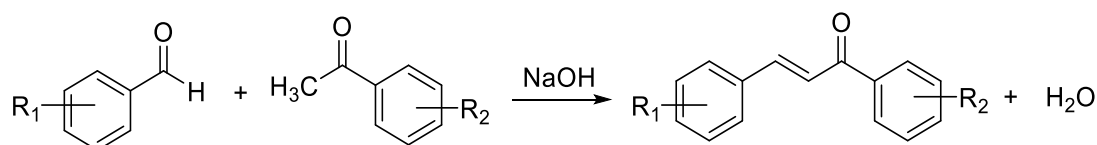


Figure 2.10: Synthesis of chalcone by solvent-free reaction

### 2.2.2 Anticancer activities of chalcone molecules

Chalcones exist in nature and can be found in plants which are commonly used as traditional folklore remedies (Żyszka et al., 2017). Chalcone derivatives play a significant role in the design and development of anticancer drugs as they have excellent activity against various cell lines (Anto et al., 1995; Boumendjel et al., 2008; Kumar et al., 2010; Mohamed et al., 2012). Some examples of the chalcone derivatives (Figure 2.11) include Sofalcone (**9**), an anti-ulcer drug that increases the amount of mucosal prostaglandin for the gastroprotective effect against *Helicobacter pylori* (Higuchi et al., 2010) while Metochalcone (**10**) was approved as a choleric drug (Sahu et al., 2012). Cucurmine (**11**) are the core structure of several drugs with a wide range of biological applications, including EGFR inhibition as well as antitumour activities (Bayomi et al., 2015; Bayomi et al., 2013; Lee et al., 2011; Manojkumar et al., 2009; Qin et al., 2017; Starok et al., 2015; Wada et al., 2015; Xu et al., 2013; Youssef et al., 2004). Butein (**12**) and Flavokawain B (**13**) are natural chalcones with anticancer activities, which were extracted from traditional Chinese medicinal herbs

(Yang et al., 2018) and the roots of *Piper methysticum* (Abu et al., 2013), respectively. Compounds **12** and **13** have been successfully utilised as EGFR inhibitors (Ji et al., 2013; Yang et al., 1998) in the development of anticancer agents.

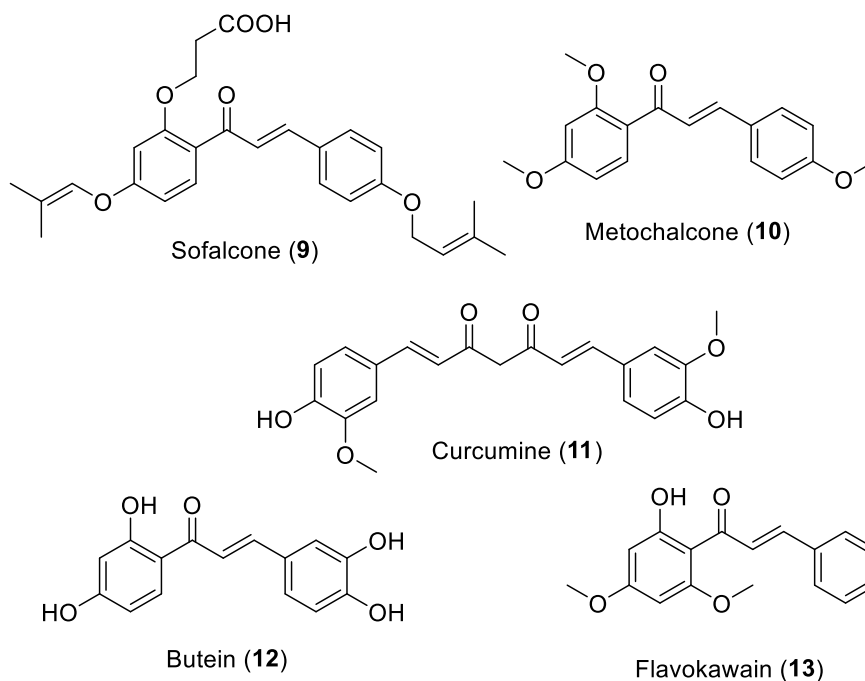


Figure 2.11: Example of drugs with chalcone scaffold

Kotra and co-workers (2010) have synthesised a new series of quinolinyl chalcone compounds **14** (Figure 2.12) which were found to possess anticancer activity (Kotra et al., 2010).

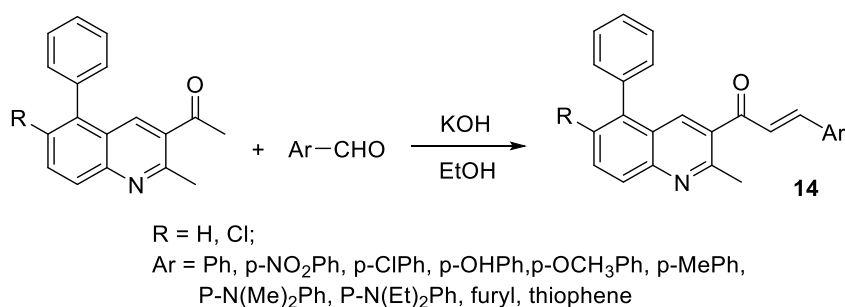


Figure 2.12: Synthesis of quinolinyl chalcone compounds **14**

Mizuno *et al.* (2010) have reported the synthesis of retinoid-chalcone hybrids **15**, as shown in Figure 2.13. The cyano-derivative (R<sub>1</sub>=CN, R<sub>2</sub>=R<sub>3</sub>=H) was identified

as an anticancer agent with an IC<sub>50</sub> value of 0.66 μM against colon cancer cell line HT-29 (Mizuno et al., 2010).

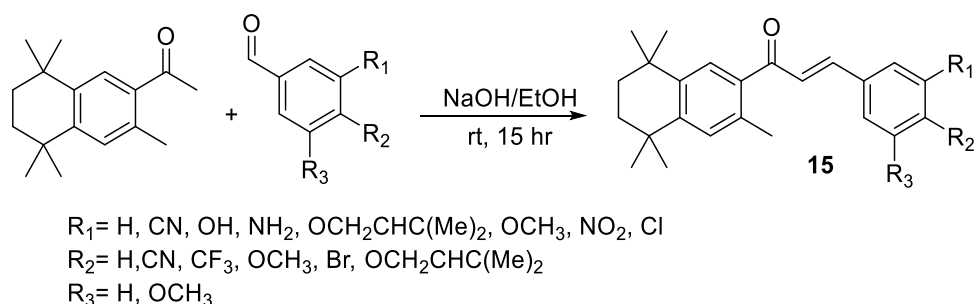


Figure 2.13: Synthesis of retinoid-chalcone hybrids **15**

Kumar et al. (2010) reported the synthesis of indolyl chalcones **16** (Figure 2.14). which were identified as anticancer agents with IC<sub>50</sub> values of 0.03 and 0.09 μM, against MIA PaCa-2 cell line.

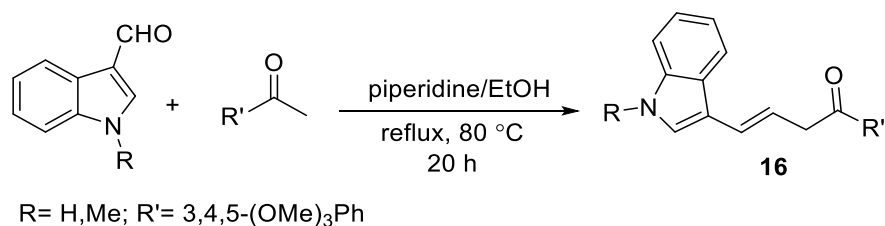


Figure 2.14: Synthesis of indolyl chalcones **16**

Syam and his co-workers (2012) have synthesised an anticancer chalcone **17**, as shown in Figure 2.15 and studied their anti-tumour activity against the MCF-7 (human breast cancer), A549 (human lung cancer), PC3 (human prostate cancer), HT-29 (colorectal cancer) and WRL-68 human normal liver cell lines. Empirical analysis revealed that most of the compounds are effective against the cancer cell lines that were tested.

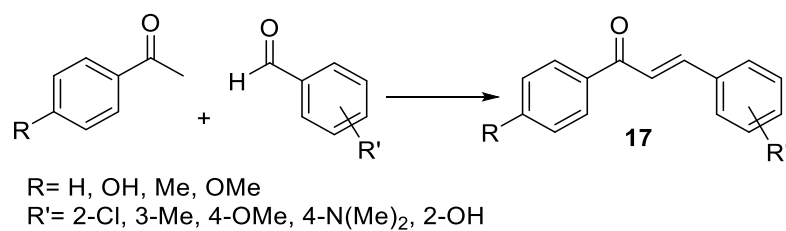


Figure 2.15: Synthesis of chalcone **17**

Ngameni et al. (2013) reported the synthesis of *O*-allyl chalcones **18** which were found to possess anticancer activity with  $\text{IC}_{50}$  values below or around  $10 \mu\text{M}$  (Figure 2.16)

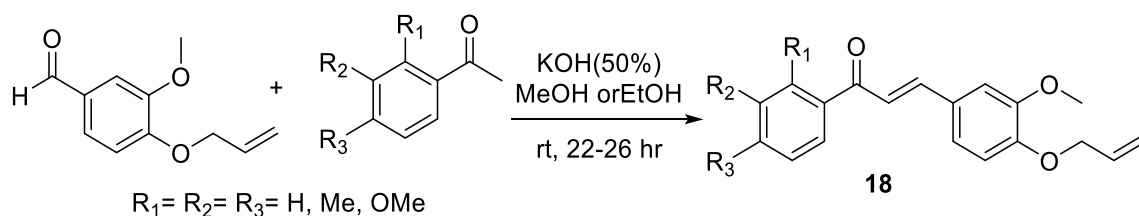
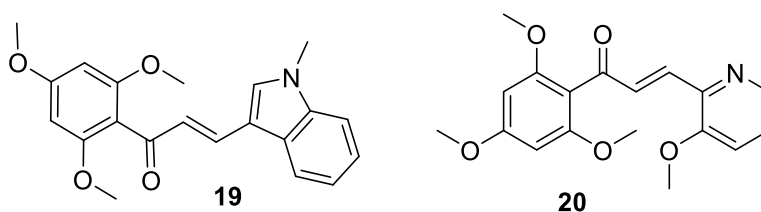
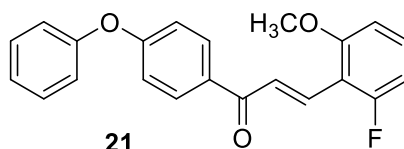


Figure 2.16: Synthesis of *O*-allyl chalcones **18**

Furthermore, Champelovier and his co-workers (2013) have reported the synthesis of compounds **19** and **20**, the cytotoxicity of both chalcones was produced by ROS generation, G2/M accumulation leading to inhibit the growth of LN229 cell. nevertheless, compound **20** caused an irreversible cell death process on both quiescent and proliferative cells, which should be considered as a possible side-effect. Compound **19** caused proliferative cell culture, which should be considered a good candidate and as a new emerging treatment targeting cell death pathways in glioblastoma cells.



Jain et al. (2014) have developed halogenated chalcone-based derivatives **21** and evaluated their anticancer activity against prostate (PC-3), ovarian (OVCAR-5), colon (COLO-205), neuroblastoma (IMR-32) and liver (HEP-2) cancer cell lines. The values were compared to the standards used (paclitaxel, adriamycin and 5-fluorouracil) and were found to show good anticancer activity ( $IC_{50} = 49.9 \mu M$ ) against COLO-205.



Ketabforoosh and his co-workers (2014) reported the synthesis of a series of chalcones **22** and flavanones **23** (Figure 2.17) and studied their anti-tumour activity against the MCF-7, MDA-MB-231 (human breast cancer), and SK-N-MC (human neuroblastoma) cell lines. The introduction of a halogen to the 3,4-dimethoxyphenyl part of both series and the attachment of a pyrrolidinyl ethoxy group on the C-7 position of the flavanone derivatives has proven to increase their activity. The 3-halogenated chalcones are more active and more potent than etoposide which was used as a standard drug against all tested cell lines.

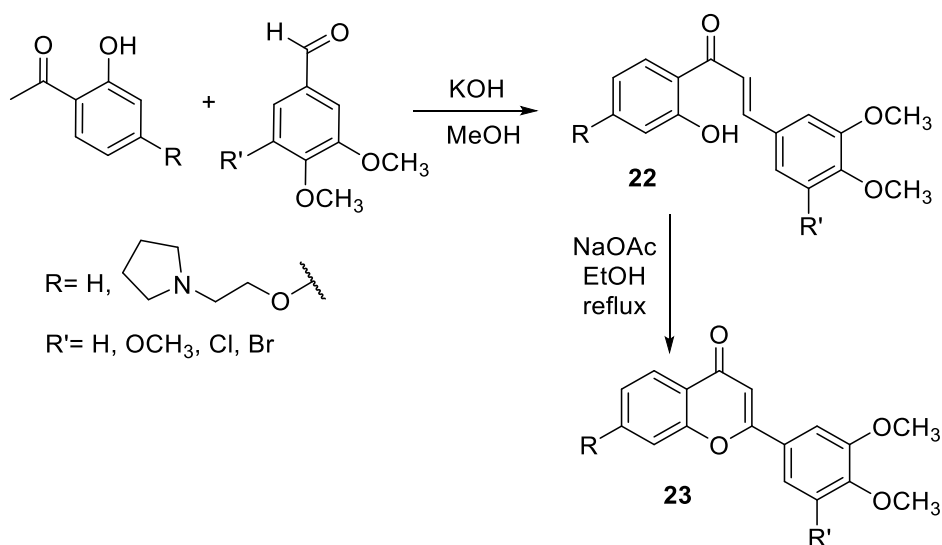
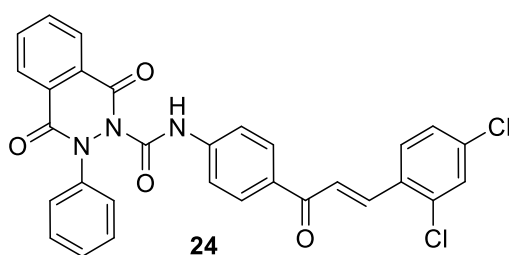


Figure 2.17: Synthesis of chalcones **22** and flavanones **23**



In 2015, El-Feky and co-workers have studied several new phthalazine-1,4-diones anticancer activity *in vitro* on HCT-116 colon cancer cells and MCF-7 breast cancer cells. Chalcone **24** was reported to be active against both cancer cell lines with the IC<sub>50</sub> values of 2.21 and 1.0 μM in colon and breast cancer, respectively, compared to the standard drug doxorubicin with the IC<sub>50</sub> values of 0.81 and 0.72 μM, respectively.



In 2015, a series of quinazolinone-chalcone derivatives **25** were synthesised by Wani and co-workers (Figure 2.18) and the compounds were found to show anticancer activity with the IC<sub>50</sub> values ranging from 5.5 to 8.5 μM against HCT-116, HL-60, PC-3, A-549, MIA PaCa-2 and MCF-7 human cell lines.

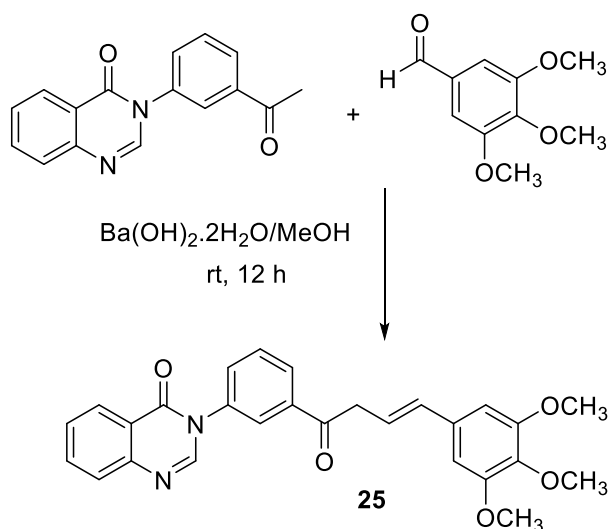


Figure 2.18: Synthesis of quinazolinone-chalcone derivatives **25**

Do and his co-workers (2016) have synthesised some heterocyclic chalcones **26** (Figure 2.19) that have cytotoxic activity with  $IC_{50} = 12.51 \mu M$ . The chalcone contains a phenothiazine moiety on the Ar ring and a thiophene heterocycle on the Ar<sub>1</sub> ring.

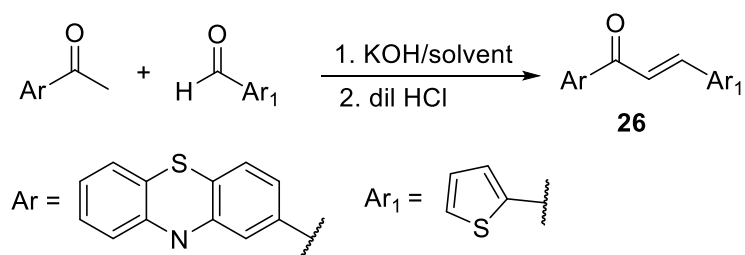


Figure 2.19: Synthesis of heterocyclic chalcones **26**

A new series of 3-aryl thiophene-2-aryl and heteroaryl chalcones **27** (Figure 2.20) were synthesised and tested *in vitro* on HCT-15 colon cancer cell lines. The best anticancer activity was shown by **27a** ( $R_1=R_3=H$ ,  $R_2=OMe$ ) and **27g** ( $R_1=H$ ,  $R_2=OMe$ ,  $R_3=2,4,6\text{-tri-Me}$ ) with  $IC_{50}$  values of  $21 \mu g/mL$  and  $22.8 \mu g/mL$ , respectively, compared to the  $IC_{50}$  value of the reference compound, doxorubicin of  $25 \mu g/mL$  (Venkataramireddy et al., 2016).

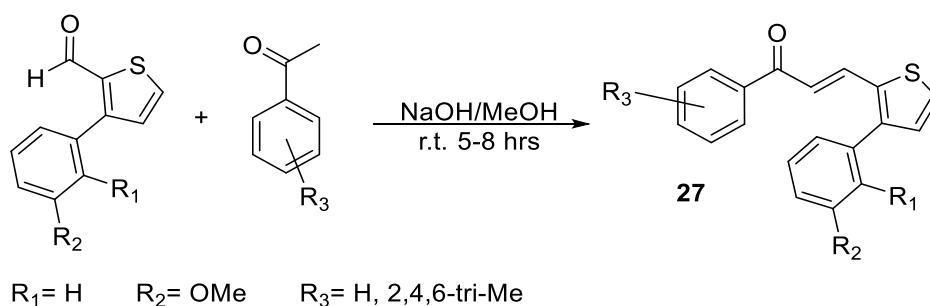
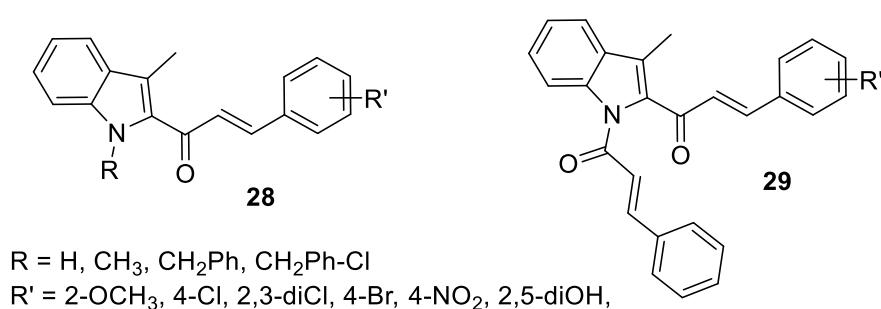


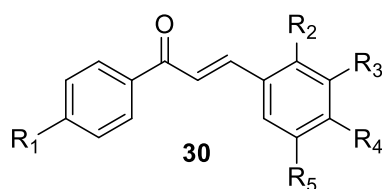
Figure 2.20: Synthesis of heteroaryl chalcones **27**

Apoptosis or programmed cell death is a natural way to remove cells that are aging from the body. There are a lot of anticancer therapies that trigger apoptosis

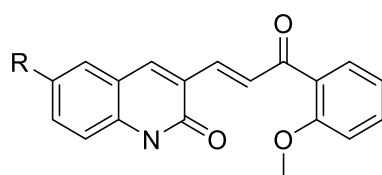
induction to kill malignant cells. However, long-term treatment with certain drugs might decline drug sensitivity in cancers which is caused by resistance. Developing new drugs to resist tumour by targeting apoptosis regulators is an attractive strategy for new cancer therapies. Zhao et al. (2017) have reported some novel indolyl-chalcone derivatives, **28** and **29** which inhibited the growth of A549 lung cancer cells effectively by causing apoptosis *in vitro* and *in vivo* with the IC<sub>50</sub> values ranging from 2.46 to 49.35 μM.



Tumour suppressor protein p53 induces cell cycle arrest and apoptotic cell death to prevent cancer development. Activation and stabilization of p53 through small organic molecules is an attractive approach for the treatment of cancers. Iftikhar *et al.* (2017) have reported a series of modified chalcones, **30** with various substituents such as chloro, fluoro, methoxy, nitro, benzyloxy, 4-methyl benzyloxy. These chalcones which were tested against human colorectal (HCT116) and breast (CAL-51) cancer cell lines revealed potent antiproliferative activities, comparable to its positive control, Nutlin-3. It was found that conjugated ketone is important for antiproliferative and p53 stabilizing activity of the chalcones. (*E*)-1-phenyl-3-(3,4,5-trimethoxyphenyl)prop-2-en-1-one **30** exhibited GI<sub>50</sub> (growth inhibition) value of  $0.473 \pm 0.043$  μM against HCT-116 cells.



In cancer therapeutic targets, four binding sites that can disrupt microtubule dynamics are taxanes, vinca alkaloids, laulimalide and colchicine. In many cancers, tubulin inhibitors target the first two sites such as paclitaxel (Tax) and vinblastine but dose-limiting toxicity and drug resistance are the issues. However, agents targeting the colchicine-binding site have minimal multidrug resistance due to high toxicity. Therefore, there is a need to develop a microtubule inhibitor that binds to the colchicine-binding site with low side effects. Chalcone-based compounds have been reported to show potent anti-tubulin activity. Since the binding of certain chalcones to tubulin can be inhibited by colchicine, they may directly bind to  $\beta$ -tubulin through the colchicine-binding pocket. Since chalcones are abundantly found in many edible fruits, they can be relatively safe to humans. Lindamulage et al. (2017) have reported some quinolone-chalcone compounds **31** with a promising activity which prefer to kill cancer over non-cancer cells. Both the compounds (R=H and R=OMe) bind to the colchicine binding pocket, leading to cell death. Importantly, both compounds (R=H and R=OMe) effectively killed the tumour cells that showed resistance to colchicine, paclitaxel and other agents. The best anticancer activity was shown by **31** (R=OMe) with  $IC_{50}$  values from 0.12  $\mu$ M (MDA-MB-468) to 1.11  $\mu$ M (U87MG).



R= H, OMe